Ghost imaging for a reflected object with a rough surface

Chunfang Wang,[1] Dawei Zhang,[1] Yanfeng Bai,[2] and Bin Chen[1,*]
[1]*University of Shanghai for Science and Technology, Shanghai 200093, China*
[2]*Department of Physics, Southeast University, Nanjing 211189, China*
(Received 8 September 2010; published 10 December 2010)

Ghost imaging for the reflected object with rough surface is investigated. The surface height variance σ_h^2 and the correlation length l_c have been introduced to characterize the rough surface. Based on a simple scattering model, we derive the analytical expressions which are used to describe the effects of σ_h^2 and l_c on ghost imaging. The results show that both σ_h^2 and l_c have no influence on the image resolution, while the convergence of the correlation decreases as σ_h^2 increases. Additionally, the bucket detector used in the test arm can dramatically improve the visibility of ghost images. The results are backed up by numerical simulations, in which a Monte Carlo approach to generate a rough surface has been used.

DOI: 10.1103/PhysRevA.82.063814 PACS number(s): 42.50.Ar, 42.30.Va, 42.30.Wb

I. INTRODUCTION

Ghost imaging is a unique method that reconstructs the image of an object by measuring the spatial correlation between a beam passing the object and a reference beam [1–5]. From the point of view of statistical optics, the ghost-imaging system retrieves the image of the object by taking advantage of the second-order correlation measurement, while most conventional imaging systems record the intensity distribution that only involves the first-order correlation properties of optical fields. The application of the high-order statistical properties of optical fields has brought some new optical phenomena since the first experimental implementation of ghost imaging in the mid-1990s [1]. Examples are quantum subwavelength Fourier-transform imaging [6] and lensless Fourier-transform imaging with incoherent light [7,8]. In recent years, more attentions have been focused on how to improve the qualities of ghost images. For instance, the spatial averaging technique is used to speed up the convergence [9,10], and high-order correlation has been exploited to enhance the visibility of ghost images [11–13].

In the previous ghost-imaging studies, the transmitted objects were usually used for its simple transmission function. In 2008, Shih *et al.* [14] reported a ghost-imaging experiment by measuring the randomly scattered and reflected light from the surface of an object, which is closer to the demands of practical imaging-sensing systems. In this paper, we investigate the performance of ghost imaging for the reflected object with rough surface. The effects of the surface height fluctuations and surface correlation length of an object on ghost imaging are discussed. During the simulations, we adopt the Monte Carlo approach to generate a rough surface. The numerical simulations according to analytical expressions are also presented at last.

II. THEORETICAL ANALYSIS

The scheme of lensless ghost imaging for the reflected object with rough surface is shown in Fig. 1. The pseudothermal source, generated by projecting a laser beam (wavelength λ) into a slowly rotating ground glass, is divided into two different paths by a nonpolarizing beam splitter. A reflected object instead of the transmitted one, is placed at a distance d_1 from the source, and the scattered light is gathered by a bucket detector which is at a distance of d_2 from the object in the test arm. An array detector with spatial resolution is put at a distance d_0 from the source in the reference arm.

For most practical applications, the random surface height $h(\alpha)$ of an object obeys the Gaussian statistics [15]. The surface is said to be wide-sense stationary, thus its height correlation function μ_h only depends on the differences of measurement coordinates [16],

$$\mu_h(\Delta\alpha) = \exp\left(-\frac{\Delta\alpha^2}{l_c^2}\right), \tag{1}$$

where $\Delta\alpha = \alpha - \alpha'$, and l_c is the surface correlation length. Light scattering from the rough surface is an extremely complex process, including single scattering, multiple scattering, shadowing, and so on. For the sake of the analysis, here we adopt a simple model which describes the relationship between the surface height fluctuations and the amplitude variations of the scattered wave. Considering a purely geometrical approximation, the scattered field $E_o(\alpha)$ just above the surface is connected to the incident field $E_i(\alpha)$ by a phase delay proportional to the height $h(\alpha)$ [16],

$$E_o(\alpha) = R(\alpha)E_i(\alpha)\exp[j\phi(\alpha)], \tag{2}$$

with

$$\phi(\alpha) = k(-\hat{i}\cdot\hat{n} + \hat{o}\cdot\hat{n})h(\alpha), \tag{3}$$

where $R(\alpha)$ represents the average amplitude reflectivity of the surface, $k = 2\pi/\lambda$ is the wave number, and the dot product $\hat{p}\cdot\hat{q}$ denotes the cosine of the angle between the unit vectors $\hat{p}$ and $\hat{q}$.

With the help of Eq. (2), under paraxial approximation, the field $E_t(x_t)$ in the detector D_t can be calculated by the Fresnel

*chenbin@usst.edu.cn.

integral [17],

$$E_t(x_t) = \frac{-1}{\lambda\sqrt{d_1 d_2}} \int E_s(x) \exp\left[-\frac{jk}{2d_1}(x - \alpha\cos\theta_i)^2\right] \times R(\alpha)\exp[j\phi(\alpha)] \times \exp\left[-\frac{jk}{2d_2}(\alpha\cos\theta_o - x_t)^2\right] dx d\alpha, \quad (4)$$

where $E_s(x)$ represents the source field, and $\theta_i(\theta_0)$ is the angle between the unit vectors $\hat{i}(\hat{o})$ and $\hat{n}$. When the object is small enough and far enough away from the source as well as the detector D_t, the angles θ_i and θ_0 can be regarded as the constants.

The field $E_r(x_r)$ in the detector D_r is given by

$$E_r(x_r) = \frac{1}{\sqrt{j\lambda d_o}} \int E_s(x') \exp\left[-\frac{jk}{2d_0}(x' - x_r)^2\right] dx'. \quad (5)$$

According to the results in Refs. [9,10], the second-order intensity correlation between the two arms has the form,

$$\begin{aligned} G(x_t,x_r) &= \langle E_t^*(x_t)E_t(x_t)E_r^*(x_r)E_r(x_r)\rangle - \langle E_t^*(x_t)E_t(x_t)\rangle\langle E_r^*(x_r)E_r(x_r)\rangle \\ &= \frac{1}{\lambda^3 d_0 d_1 d_2} \int \langle E_s(x)E_s^*(x''')\rangle\langle E_s(x')E_s^*(x'')\rangle R(\alpha)R^*(\alpha')\langle\exp\{j[\phi(\alpha) - \phi(\alpha')]\}\rangle \\ &\quad \times \exp\left\{\frac{jk}{2d_1}[(x - \alpha\cos\theta_i)^2 - (x'' - \alpha'\cos\theta_i)^2]\right\} \exp\left\{\frac{jk}{2d_0}[(x' - x_r)^2 - (x''' - x_r)^2]\right\} \\ &\quad \times \exp\left\{\frac{jk}{2d_2}[(\alpha\cos\theta_o - x_t)^2 - (\alpha'\cos\theta_o - x_t)^2]\right\} dx dx' dx'' dx''' d\alpha d\alpha', \end{aligned} \quad (6)$$

where we have assumed that the statistics of the source and the surface height fluctuations are independent of each other.

In terms of Ref. [16], the statistical average of phase exponential caused by the rough surface can be written as

$$\begin{aligned} \langle\exp\{j[\phi(\alpha) - \phi(\alpha')]\}\rangle &= \exp\left\{-\sigma_\phi^2[1 - \mu_h(\Delta\alpha)]\right\} \\ &= \exp\left\{-\sigma_\phi^2\left[1 - e^{-\frac{\Delta\alpha^2}{l_c^2}}\right]\right\}, \end{aligned} \quad (7)$$

where σ_ϕ^2 is the variance of phase, which is related to the variance of the surface height fluctuations σ_h^2 through

$$\sigma_\phi^2 = [k(-\hat{i}\cdot\hat{n} + \hat{o}\cdot\hat{n})]^2\sigma_h^2, \quad (8)$$

We suppose that the source is fully spatially incoherent and its intensity distribution is of the Gaussian type, and then the first-order correlation function of the source has the form,

$$\langle E_s(x)E_s^*(x')\rangle = I_0 \exp\left(-\frac{x^2}{r_e^2}\right)\delta(x - x'), \quad (9)$$

where I_0 denotes the mean intensity at the center of the source, and r_e is the radius at which the mean intensity falls to $1/e$.

To get the ghost image of the object, D_r is placed at a distance $d_0 = d_1$. Substituting Eqs. (7) and (9) into Eq. (6), we can obtain the following expression:

$$\begin{aligned} G(x_t,x_r) = \frac{I_0^2}{\lambda^3 d_0 d_1 d_2} \int R(\alpha)R^*(\alpha') \exp\left\{-\sigma_\phi^2\left[1 - e^{-\frac{\Delta\alpha^2}{l_c^2}}\right]\right\} \\ \times \exp\left\{\frac{jk}{2d_1}\cos\theta_i^2(\alpha^2 - \alpha'^2)]\right\} \exp\left\{\frac{jk}{2d_2}\left[\cos\theta_o^2\right.\right. \\ \left.\left. \times (\alpha^2 - \alpha'^2) + 2x_t\cos\theta_o(\alpha' - \alpha)\right]\right\} \\ \times h_g(\alpha,\alpha',x_r)\, d\alpha d\alpha', \end{aligned} \quad (10)$$

with

$$\begin{aligned} h_g(\alpha,\alpha',x_r) &= \int \exp\left(-\frac{x^2 + x'^2}{r_e^2}\right) \\ &\exp\left\{\frac{jk}{2d_1}[2x(x_r - \alpha\cos\theta_i) + 2x'(\alpha'\cos\theta_i - x_r)]\right\} dx dx' \\ &= \pi r_e^2 \exp\left\{-\frac{k^2 r_e^2}{4d_1^2}[(x_r - \alpha\cos\theta_i)^2 + (x_r - \alpha'\cos\theta_i)^2]\right\}, \end{aligned} \quad (11)$$

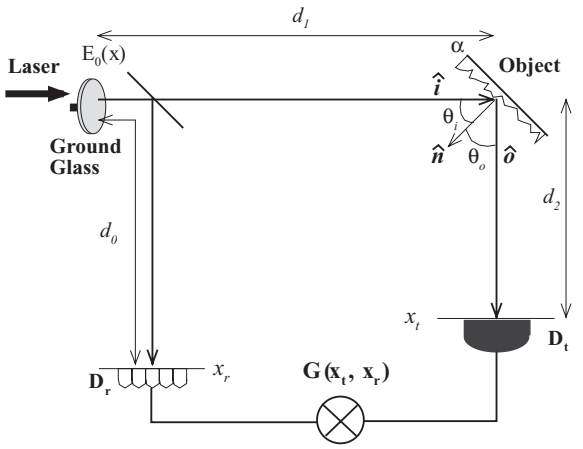

FIG. 1. The scheme of lensless ghost imaging for the reflected object with rough surface. $\hat{n}$ represents a unit vector pointing in the direction of the average surface normal, $\hat{i}$ denotes a unit vector pointing in the direction of incidence of the illumination, and $\hat{o}$ corresponds a unit vector pointing in the direction of the detection plane.

where the identity $\int_{-\infty}^{+\infty}\exp(-ax^2+bx)dx=(\pi/a)^{1/2}\exp(-b^2/4a)$ has been used in the calculation. Eq. (11) corresponds to the correlation result in the case of D_t being a point detector. In this case, the image of the object can be hardly extracted from the correlation function due to the surface height fluctuations. To solve this problem, the bucket detector can be used in the test arm, and by integrating over x_t, Eq. (10) becomes

$$\begin{aligned}G(x_r)&=\int dx_t G(x_t,x_r)\\&=\frac{I_0^2}{\lambda^2 d_0 d_1\cos\theta_o}\int\delta(\alpha-\alpha')R(\alpha)R^*(\alpha')\\&\quad\times\exp\left\{-\sigma_\phi^2\left[1-e^{\frac{\Delta\alpha^2}{l_c^2}}\right]\right\}\exp\left\{\frac{jk}{2d_1}\left[\cos\theta_i^2(\alpha^2-\alpha'^2)\right]\right.\\&\quad\left.+\frac{jk}{2d_2}\left[\cos\theta_o^2(\alpha^2-\alpha'^2)\right]\right\}h_g(\alpha,\alpha',x_r)\,d\alpha d\alpha'\\&=\frac{\pi I_0^2 r_e^2}{\lambda^2 d_0 d_1\cos\theta_o}\int|R(\alpha)|^2\\&\quad\times\exp\left\{-\frac{k^2 r_e^2}{2d_1^2}[(x_r-\alpha\cos\theta_i)^2]\right\}d\alpha,\end{aligned}\tag{12}$$

where the factor associated with the surface height variance σ_h^2 and correlation length l_c has been eliminated. Equation (12) also shows that the reconstruction of images doesn't depend on the detection direction (characterized by θ_o) of the bucket detector, which is just used to collect the reflected light from the object. However, the incident angle θ_i will induce a magnification factor of $\cos\theta_i$. So, the surface properties of the object almost have no influence on the image resolution.

In simulations, a random rough surface can be generated by the Monte Carlo approach. The surface height $h(\alpha)$ is considered as the superposition of a series of independent harmonic waves with amplitudes obeying Gaussian statistics [15],

$$h(\alpha_n)=\frac{1}{L}\sum_{m=-M/2}^{M/2-1}F(K_m)\exp(jK_m\alpha_n),\tag{13}$$

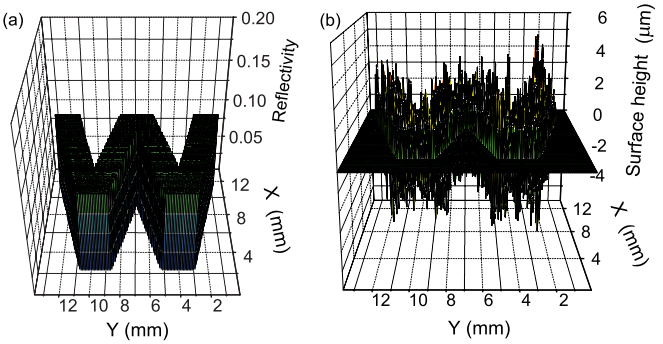

FIG. 2. (Color online) A refelcted object with the rough surface. (a) is the average amplitude reflectivity of the surface; (b) shows the surface height fluctuations.

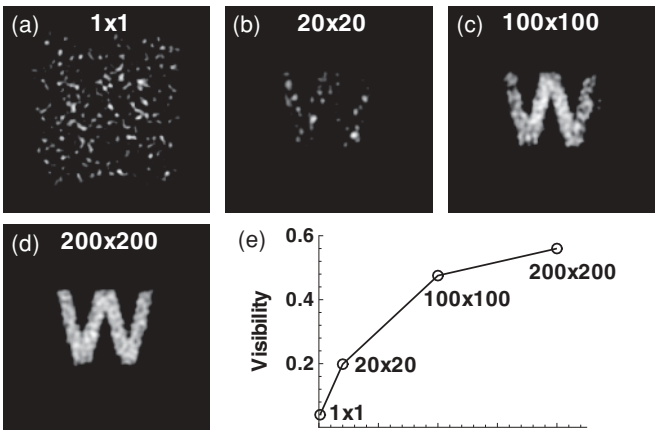

FIG. 3. The reconstructed images through the correlation. (a) A point detector case in the test arm. (b)–(d) Correspond to the bucket detector cases 20 × 20, 100 × 100, and 200 × 200 sample points via summing over, respectively. The visibility of the images (a)–(d) is plotted in (e). Statistical over 20 000 pulsed shots.

where $\alpha_n=n\Delta\alpha(n=1,2,\ldots N)$ is the n^{th} discrete space point on the surface, $L=\Delta\alpha\,M$, $K_m=2\pi m/L$, and $F(K_m)$ which represents the Fourier transform of $h(\alpha_n)$ is defined as

$$F(K_m)=\sqrt{2\pi L W(K_m)}\times\begin{cases}[N(0,1)+jN(0,1)]/\sqrt{2}, & m\neq 0,M/2,\\ N(0,1), & m=0,M/2,\end{cases}\tag{14}$$

where $W(K_m)$ is the roughness spectral density and each $N(0,1)$ indicates an independent Gaussian random variable with zero mean and unit variance. For most objects, the roughness spectrum of the surface height satisfying Gaussian statistics has the form [15],

$$W(K)=\frac{\sigma_h^2 l_c}{2\pi}\exp\left\{\frac{-Kl_c^2}{4}\right\}.\tag{15}$$

Taking Eqs. (14) and (15) into Eq. (13), the surface height distribution can be obtained by a fast Fourier transform (FFT).

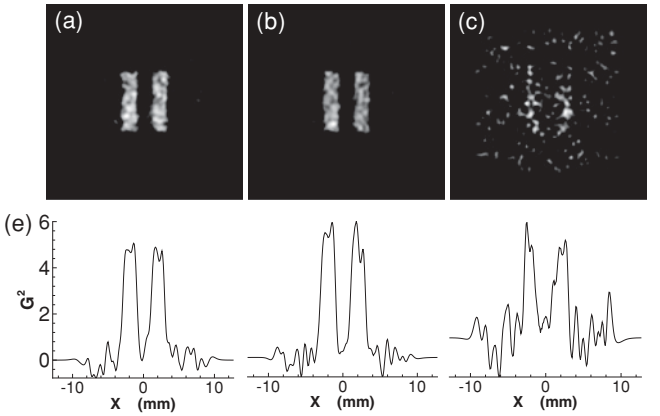

FIG. 4. The images of the double slit are reconstructed under the conditions of (a) $\sigma_h=\lambda$, (b) $\sigma_h=5\lambda$, (c) $\sigma_h=10\lambda$, respectively. Statistics over 10 000 pulsed shots.

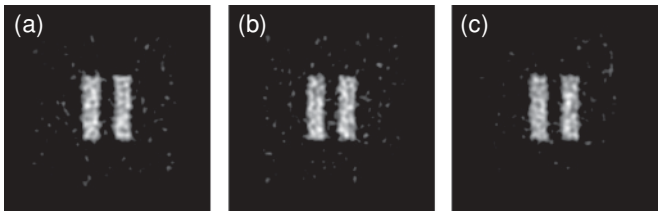

FIG. 5. The images of the double slit are reconstructed under (a) $l_c = \lambda$, (b) $l_c = 5\lambda$, (c) $l_c = 10\lambda$, respectively. Statistics over 10 000 pulsed shots.

III. NUMERICAL SIMULATION

Now, let us consider the setup of ghost imaging for the reflected object displayed in Fig. 1. A pulsed laser beam with a mean wavelength $\lambda = 632.8$ nm and a diameter $D = 2r_e = 3$ mm illuminates the ground glass, and the pseudothermal field is described by a grid of 256×256 with a sample spacing $\Delta x = \Delta y = 0.1$ mm. The relevant distances are set as $d_0 = d_1 = 3$ m and $d_2 = 2$ m. First, a reflected object (letter "**W**") has been created according to Eq. (13). Figure 2(a) corresponds to the average amplitude reflectivity of the surface with $R(\alpha) = 0.1$, and Fig. 2(b) shows the surface height fluctuations. The surface correlation length and height variance are $l_c = 5\lambda$ and $\sigma_h = 2\lambda$, respectively. The incident angle and the reflection angle are chosen as $\theta_i = 30^\circ$ and $\theta_o = 60^\circ$, respectively.

In the simulations, the image of the object cannot be obtained by using a point detector in the test arm [see Fig. 3(a)]. When D_t is used as a bucket detector, Figs. 3(b)–3(d) are reconstructed via summing over 20×20, 100×100, and 200×200 sample points in D_t, respectively. We find that the visibility, defined as [18]

$$\text{Visibility} = \frac{G_{\max} - G_{\min}}{G_{\max} + G_{\min}}, \tag{16}$$

is improved with the increase of the detection area (i.e., the number of sample point), as shown in Fig. 3(e).

To investigate the influences of the surface height variance and correlation length on ghost images, we select a double slit with rough surface in simulations. First of all, keeping $l_c = 5\lambda$ invariant, the images of the double slit are reconstructed under $\sigma_h =$ (a) λ, (b) 5λ, and (c) 10λ, as shown in Fig. 4. The numerical results show that σ_h has no obvious influences on the resolution, but the convergence of the correlation decreases when σ_h increases to a certain degree.

And then with the same $\sigma_h = 5\lambda$, we reconstruct the images of the double slit (see Fig. 5) with the same $\sigma_h = 5\lambda$ under $l_c = \lambda$, 5λ, and 10λ, respectively. There seems to be little difference between Figs. 5(a)–5(c), which indicates that l_c does not affect either the image resolution or the convergence of the correlation.

IV. CONCLUSION

In summary, we have derived the analytical expression describing ghost imaging for the reflected object with rough surface. The results show that the surface height variance and correlation length barely affect the imaging resolution when the bucket detector is used in the test arm. In the simulations, by using the Monte Carlo method, we generate two-dimensional random arrays of height values, which have the same statistics as the surface height fluctuations of the object. The numerical results show that the visibility of the image increases with the increase of the detecting area of the bucket detector in the test arm, the convergence of the correlation decrease as the surface height variance is large enough, and the surface correlation length almost has no effect on the qualities of images. It should be noted that the analytical calculations and the numerical results given in the paper are based on a simple geometrical approximation. In fact, the light scattering from the rough surface is more complicated, and further studies will be considered in future works.

ACKNOWLEDGMENTS

Support from the National Natural Science Foundation of China (Grants No. 10774035, No. 10904015, and No. 60908021) and the innovation Program of Shanghai Municipal Education Commission (Grant No. 11YZ118), the Shanghai Committee of Science and Technology (Grants No. 09QA1404200, No. 1052nm07100, and No. 10DZ2273800) is also acknowledged.

[1] T. B. Pittman, Y. H. Shih, D. V. Strekalov, and A. V. Sergienko, Phys. Rev. A **52**, 3429(R) (1995).
[2] A. Gatti, E. Brambilla, L. A. Lugiato, and M. I. Kolobov, Phys. Rev. Lett. **83**, 1763 (1999).
[3] R. S. Bennink, S. J. Bentley, and R. W. Boyd, Phys. Rev. Lett. **89**, 113601 (2002).
[4] G. Scarcelli, A. Valencia, and Y. Shih, Phys. Rev. A **70**, 051802(R) (2004).
[5] Y.-H. Zhai, X.-H. Chen, D. Zhang, and L.-A. Wu, Phys. Rev. A **72**, 043805 (2005).
[6] M. H. Zhang, Q. Wei, X. Shen, Y. Liu, H. Liu, Y. Bai, and S. Han, Phys. Lett. A **366**, 569 (2007).
[7] J. Cheng, and S. S. Han, Phys. Rev. Lett. **92**, 093903 (2004).
[8] M. H. Zhang, Q. Wei, X. Shen, Y. F. Liu, H. L. Liu, J. Cheng, and S. S. Han, Phys. Rev. A **75**, 021803 (2007).
[9] M. Bache, E. Brambilla, A. Gatti, and L. A. Lugiato, Phys. Rev. A **70**, 023823 (2004).
[10] M. Bache, E. Brambilla, A. Gatti, and L. A. Lugiato, Opt. Express **12**, 6067 (2004).
[11] Y. F. Bai and S. S. Han, Phys. Rev. A **76**, 043828 (2007).
[12] K. W. C. Chan, M. N. O'Sullivan, and R. W. Boyd, Opt. Lett. **34**, 3343 (2009).
[13] I. N. Agafonov, M. V. Chekhova, T. Sh. Iskhakov, and L.-A. Wu, J. Mod. Opt. **56**, 422 (2009).
[14] R. Meyers, K. S. Deacon, and Y. Shih, Phys. Rev. A **77**, 041801(R) (2008).
[15] E. I. Thorsos, J. Acoust. Soc. Am. **83**, 78 (1988).
[16] J. W. Goodman, in *Speckle Phenomena in Optics: Theory and Applications*, Version 6.1 (Roberts and Company, Greenwood Village, 2007), pp. 83–87.
[17] J. W. Goodman, *Introduction to Fourier Optics* (McGraw-Hill, New York, 1968).
[18] M. O. Scully and M. S. Zubairy, *Quantum Optics* (Cambridge University Press, Cambridge, 1997).